



HAL
open science

Removal of cerium ions by Amino Cyclohexyl Phosphonic Acid (ACHPA) intercalated into layered double hydroxide (Ni/Al-LDH)

M. Kadari, M. Makhlouf, M. Kaid, Z. Benmaamar, Didier Villemin

► To cite this version:

M. Kadari, M. Makhlouf, M. Kaid, Z. Benmaamar, Didier Villemin. Removal of cerium ions by Amino Cyclohexyl Phosphonic Acid (ACHPA) intercalated into layered double hydroxide (Ni/Al-LDH). *Advances in Materials and Processing Technologies*, 2022, pp.1-13. 10.1080/2374068X.2022.2144209 . hal-03871195

HAL Id: hal-03871195


<https://hal.science/hal-03871195v1>

Submitted on 25 Nov 2022

HAL is a multi-disciplinary open access archive for the deposit and dissemination of scientific research documents, whether they are published or not. The documents may come from teaching and research institutions in France or abroad, or from public or private research centers.

L'archive ouverte pluridisciplinaire **HAL**, est destinée au dépôt et à la diffusion de documents scientifiques de niveau recherche, publiés ou non, émanant des établissements d'enseignement et de recherche français ou étrangers, des laboratoires publics ou privés.

Removal of cerium ions by Amino Cyclohexyl Phosphonic Acid (ACHPA) intercalated into layered double hydroxide (Ni/Al-LDH)

M. Kadari ^a, M. Makhlouf ^a, M. Kaid^b, Z. Benmaamar ^a and D. Villemin ^c

^aFundamental and Apply Physics Laboratory FUNDAPL, Blida 1, Algeria; ^bDepartment of Chemistry, University D^r Moulay Taher, Saida, Algeria; ^cLaboratoire de Chimie Moléculaire et Thio-organique, UMR CNRS 6507, INC3M, FR 3038, ENSICAEN & Centre de Recherche, Université de Caen, Caen, France

ABSTRACT

Amino phosphonic acids are good heavy metal extractants for liquid–liquid extraction, but this method requires the use of an organic solvent, which is itself a pollutant. The incorporation of these acids in solid supports gave us the opportunity to find a solution to this problem. The synthesis of the new material by incorporation of Amino-Cyclo-Hexyl Phosphonic Acid into the inter-layer space of the Ni/Al-LDH, designated as Ni/Al-ACHPA, was carried out by the coprecipitation method and anion exchange. The new hybrid material was characterised by FTIR, XRD and BET. The results obtained show that ACHPA is well intercalated in LDH. The adsorption performance of the new hybrid material towards the ions of Cerium Ce^{+3} , has been investigated under different parameters. Under optimal conditions, where the highest recovery (75%) was obtained at pH 6 using 0.1 g of adsorbent (Ni/Al-ACHPA) for less than 30 min of agitation. The modelling results of the kinetics indicate that the Ce^{+3} adsorption process mechanism is well fitted by a pseudo-second order equation with a high regression coefficient ($R^2 = 99\%$) and the adsorption isotherms were fitting well with the Freundlich isotherm model.

1. Introduction

Amino-Phosphonic acids have shown an inherent advantage in being used as an effective adsorbent and chelating ligand [1] in the adsorption of toxic heavy metals due to their remarkable physicochemical properties [2]. Amino phosphonic acids are chelating agents [3,4] which are synthesised by a Mannich reaction (Figure 1), this reaction is one of the best methods for introducing the amine function into organic molecules [5–7].

The enormous progress made in the synthesis of amino-phosphonic acids, especially Amino-Cyclo-Hexyl-phosphonic acid ACHPA (Figure 2), is due to the importance of their applications on an industrial scale, especially in liquid–liquid extraction processes [8]. These extractants are characterised by their active centre, which is formed by

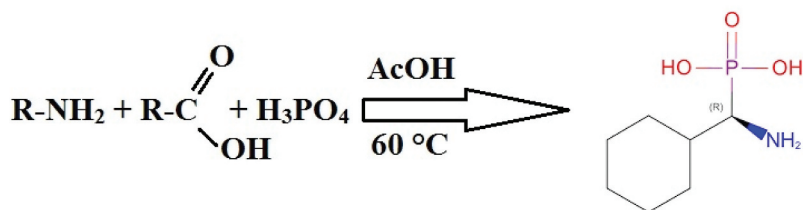


Figure 1. Mannich-type reaction.

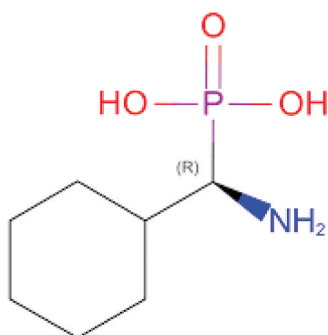


Figure 2. Structural unit of Amino-Cyclo-Hexyl-Phosphonic Acid (ACHPA).

a phosphorus atom (P) linked, on one side, by a double bond to an oxygen atom (=O) and, on the other side, by an alkyl group (–R).

The use of these phosphonic acids for the extraction of heavy metals requires an organic solvent, but the latter is a pollutant for the environment [9,10], which forced us to replace the organic solvent with adsorbents such as layered double hydroxide LDH.

Layered double hydroxide results from the succession and stacking of sheets, generally of inorganic nature. These two-dimensional lamellar compounds exhibit a high anisotropy of their chemical bonds, strong within the hydroxylated sheets [11,12], weak for the cohesion of the sheets between them. This peculiarity allows the incorporation in the interlayer space of a wide variety of anions [13].

The three usual methods designed for the synthesis of layered double hydroxide are the co-precipitation [14] method, the anion exchange method [15] and the reconstruction method [16]. The direct co-precipitation method is the most used method for the layered double hydroxide preparation. It consists in simultaneously precipitating the metal cations, by adding a basic solution to a solution of chloride or nitrate salts taken in adequate proportions.

In this work, we were interested in synthesising a new hybrid material by grafting a good chelating agent in a solid support, such as layered double hydroxides, in addition to the study of the adsorptive performance of this new material (Ni/Al-ACHPA) on the removal of Ce^{+3} ions in aqueous solution (Figure 3).

In toxicology, Cerium as heavy metals can be defined as metals of a cumulative nature having essentially very harmful effects on living organisms. Being this poisonous metals presence in water sources at levels higher than the permissible amounts can affect

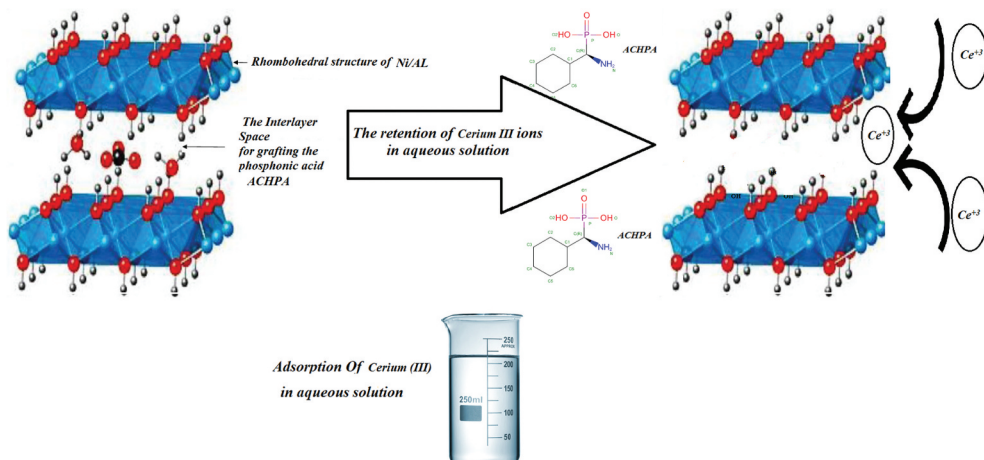


Figure 3. Graphical abstract.

humans and animals health [17] and can cause various illnesses like brain damage, chest pain, shortness of breath, vomiting, fever and skin rashes, diarrhoea, asthma, hypotension, liver and thyroid damage, allergies, and bone defects [18–20].

Cerium is the most abundant element of the lanthanides (approximately 0.0046% of the earth's crust) and the most reactive with the exception of Europium [21]. Human activities may end up with these toxic elements in the hydrosphere, as well as the food cycle and the ecosystem [22].

2. Materials and methods

2.1. Synthesis of Ni/Al- CO_3

Layered double hydroxide (Ni-Al- CO_3) was obtained by a co-precipitation method at constant pH [23]. For this purpose two solutions have been prepared (Solution A and Solution B): (A) 0.75 mol/l $Ni(NO_3)_2 \cdot 6H_2O$ and 0.25 mol/l of $Al(NO_3)_3 \cdot 9H_2O$ were dissolved in 250 ml of distilled water and (B) 2 mol/l solution of Na_2CO_3 was dissolved in 250 ml of distilled water.

Both solutions were heated to 353 K. One hundred millilitres of H_2O heated to 353 K was introduced into a three-neck flask, and a small amount of the carbonate solution was added to the two solutions mixture (A and B) previously prepared, in order to obtain a pH = 8. The two solutions were then introduced into the container, carefully controlling the rate of addition in order to maintain the pH between 9 and 10. After the completion of the precipitation, the suspension was aged at the same temperature for 60 min.

The precipitate was filtered, and the solid obtained was washed several times with distilled water in order to remove excess ions (NO_3^- , Na^+ , etc.). The material, noted LDH, is dried at 383 K for 18 h and was crushed

2.2. Synthesis of Ni/Al-ACHPA

Layered double hydroxides are bilayer compounds with exchangeable anions in the interlayer space, which makes it possible to exchange these anions with negatively charged compounds such as phosphonic acids in solution [24].

For this, a mass of 20 g of Ni/Al-CO₃ was brought into contact with 100 ml of distilled water and 1 g of acid dissolved in 100 ml of distilled water (1/20). The two solutions were mixed and stirred for 24 h. The mixture was filtered and then dried at 383 K.

2.3. Characterization

A Shimadzu brand UV-2401PC spectrophotometer was used for the analysis of the concentration of Ce⁺³ in aqueous solution. In order to achieve a calibration line that will allow us to determine the concentration of the remaining Ce⁺³ ions after adsorption, we prepared solutions of Cerium nitrate Ce(NO₃)₃ · 6H₂O at different concentrations [10⁻⁶ to 10⁻⁴M]. The calibration curve (absorbance as a function of the concentration of Ce⁺³ obtained after linear regression of the experimental points exhibited good linearity (regression coefficient is 0.9988). The parameters (R and R²) obtained show a strong correlation between the values of the absorbance ratios and the concentration ratios used to draw the calibration line.

X-ray diffraction spectra (xRD) is obtained using a PANAnalytical X'PERT Pro diffractometers. The reflection mode is 40 KV with CuKα radiation (1.5405) and a scan of 2θ from 5 to 100.

The Ni/Al-CO₃ and Ni/Al-ACHPA infrared spectra are obtained using a Perkin-Elmer 16 PC Fourier Transform FTIR spectrophotometer equipped with a thermostat.

The BET Brunauer–Emmett–Teller method was used to determine the specific surface area and pore size. The measurements were found by adsorption and desorption of N₂ at 77 K and the results are collected and processed by Quanta Chromium Autosorb-6.

3. Results and discussions

3.1. Characterization results

This study is not intended to perform a refinement of the structural parameters by the so-called Rietveld-type method (study requiring the precise measurement of the intensity of each line) but only to ensure the crystallographic structure of each sample and to specify globally the lattice parameters for the structure studied. For this, the diffraction lines positions as a function of the angle 2θ are sufficient and make it possible to attribute to each reflection a Miller index triplet (hkl) characteristic of the diffracted plane.

X-ray diffractograms of Ni/Al-CO₃ and Ni/Al-ACHPA phases show a general appearance characteristic of the type phases of layered double hydroxide within particular, the appearance of all the harmonic lines (001) encountered in isotype compounds with a lamellar structure and indicate a hexagonal network, with a rhombohedral symmetry typically R-3m.

Diffractograms of hydrotalcite Ni/Al-CO₃ and Ni/Al-ACHPA compounds show many fine, intense and symmetrical reflections at low values of 2θ for the planes (003), (006), (110), (113) and wider, less intense and asymmetrical at wide angles. We note that almost

no specific changes were made in the XRD spectrum provided for the desired LDH before and after the grafting process using ACHPA, this is probably justified by the strongly low amount of ACHPA compared to LDH.

The Ni/Al- CO_3 X-ray diffractogram (Figure 4), the measured inter-lamellar distance is relative to the presence of small anions in the inter-leaf spaces such as the CO_3^{2-} ions and is in agreement with those of literature [25,26]. The parameter (a) giving the distance between two neighbouring metals is good, which explains why the synthesised structure has shown layered double hydroxide precursors, which were successfully synthesised. The basal distance is 7.78 Å indicating that the water is well intercalated in the inter-leaf spaces. The width of the lines observed indicates a good crystallinity of the phase, which allows the fine resolution of the structures of the compounds intercalated by different levels of carbonate anions.

Figure 4, the Ni/Al-ACHPA X-ray diffractogram showed that the inter-leaf space increased from 7.72 to 7.78 Å, which indicates that the Amino-Cyclo-Hexyl-phosphonic acid ACHPA is well intercalated successfully. In comparison of full width at half height (FWHM) of peaks for two samples, Ni/Al-ACHPA showed a wider reflection than Ni/Al- CO_3 revealing weaker crystallinity [27–29]. The results of the X-ray diffraction analysis of Ni/Al- CO_3 and Ni/Al-ACHPA are shown in Table 1.

Infrared radiation (FTIR) is located in the part of the electromagnetic spectrum between the visible region and that of the microwaves [22]. This gives a spectrum in percentage of energy absorbed as a function of wavelength. The peaks observed correspond to the energies absorbed for atomic bonds whose energy varies according to the

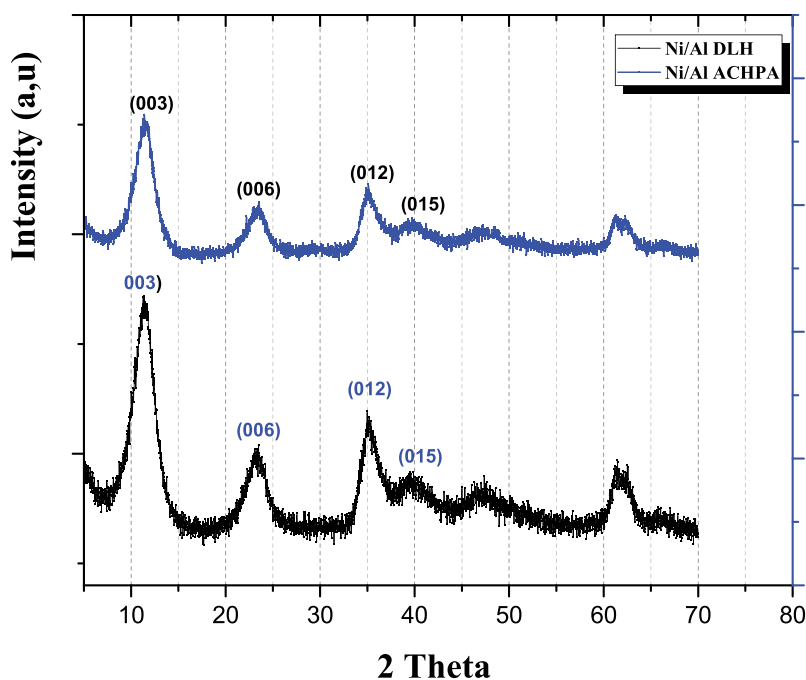
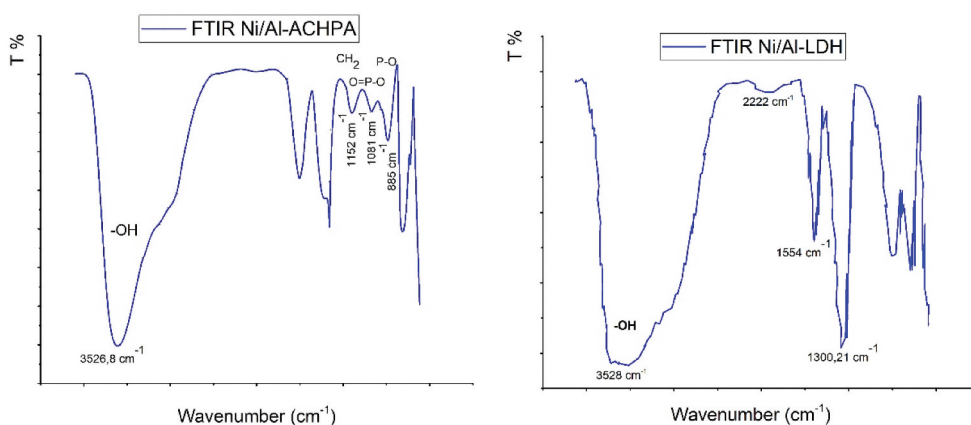


Figure 4. XRD pattern of Ni/Al HDL and Ni/Al-ACHPA.

Table 1. Peak list of DRX of Ni/Al-CO₃ and Ni/Al-ACHPA.

Peak	The cell parameters of Ni/Al-CO ₃			The cell parameters of Ni/Al-ACHPA		
	hkl	d _{hkl} (Å)	2θ	hkl	d _{hkl} (Å)	2θ
1	003	7.7283	11.37	003	7.7817	11.45
2	006	3.7742	23.57	006	3.8119	23.34
3	012	2.5549	35.13	012	2.5563	35.11
4	015	2.2687	39.73	015	1.9141	47.50
5	018	1.9208	47.33	018	1.5079	61.50

**Figure 5.** FTIR Ni/Al-ACHPA and Ni/Al-LDH.

environment. The identification of these absorption bands makes it possible to obtain the chemical functions present in the product analysed.

FT-IR spectra were used to confirm the intercalation of Amino-Cyclo-Hexyl Phosphonic Acid ACHPA in the layers of the double lamellar hydroxide, the results are shown in Figure 5. A wide band around 3528 cm⁻¹ and 3526.8 cm⁻¹ was attributed to the vibrations of OH in inter-lamellar water molecules. The two peaks around 1152 cm⁻¹ and 1081 cm⁻¹ were attributed to the two functional groups -CH₂ and O=P-OH of ACHPA and the peaks around 885 cm⁻¹ and 900 cm⁻¹ were attributed to the P-O function of the phosphonic acid [27–29].

Figure 6, shows the nitrogen adsorption/desorption isotherms for Ni/Al-LDH and the new hybrid material Ni/Al-ACHPA. The shape of the isotherms is of the same type (IV) according to the IUPAC classification with systematic hysteresis for the two compounds Ni/Al-CO₃ and N/Al-ACHPA, highlighting the mesoporous nature of these materials. Associated parameters such as special surface area (S_{BET}), total pore volume (V_t) and average pore diameter (D_a) are also presented in Figure 6.

3.2. Parametric study

3.2.1. Equilibrium time

Since adsorption is a process of transferring pollutant from the liquid phase to the solid phase, the time between the two phases acts as a limiting factor. The effect of the contact time between the two phases, adsorbent-adsorbate, is an important parameter in all

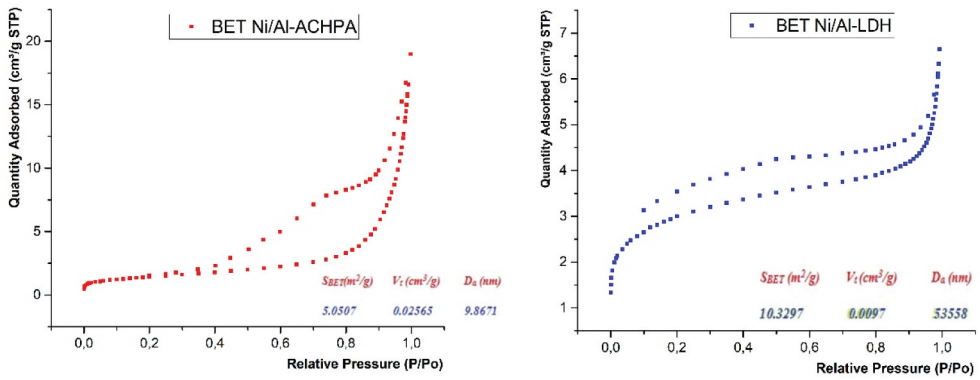


Figure 6. Nitrogen adsorption-desorption isotherms and corresponding pore size distributions.

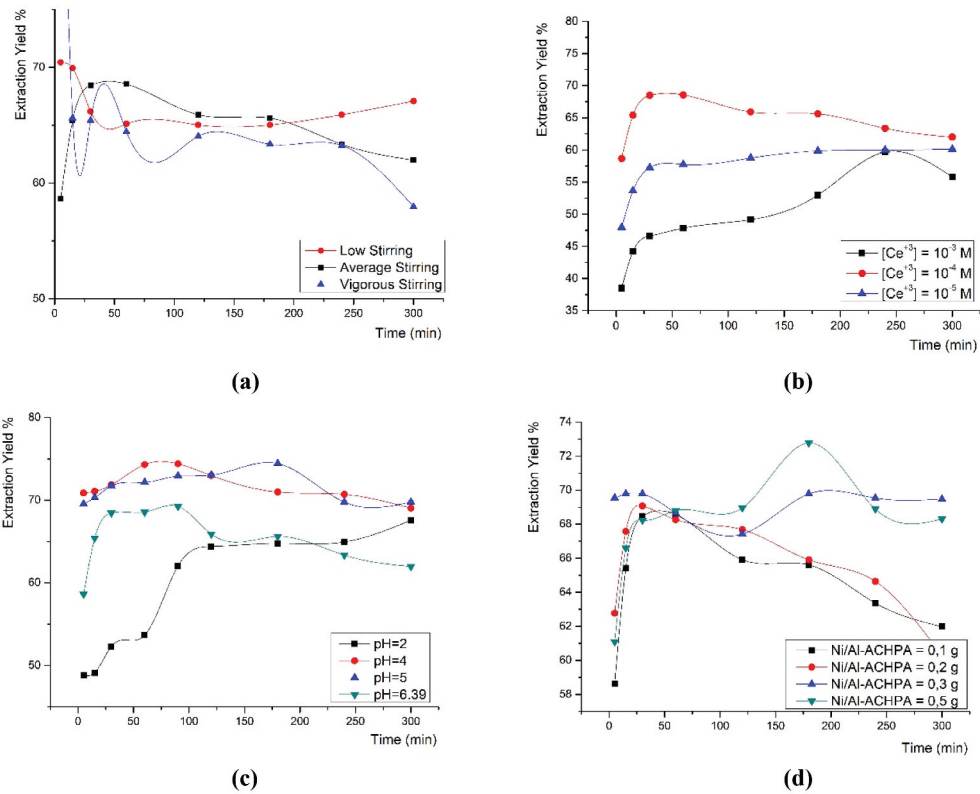


Figure 7. Parametric study: (a) Equilibrium time, (b) Effect of the initial concentration of Ce³⁺, (c) pH effect, (d) Effect of the amount of hybrid material (Ni/Al-ACHPA).

extraction processes. In order to determine the equilibrium time, the transfer kinetics of the Ce³⁺ solute from one phase to another (Ni/Al-ACHPA) were performed until equilibrium was reached. The results obtained are shown in Figure 7.

Strong stirring gave us maximum performance after just 5 min, then a drastic drop caused by the desorption of cations under the effect of the stirring speed. The average speed is interesting because a plateau is obtained for up to 200 min with 65% [30,31].

Stirring speed is a physical condition, which is not related to the chemical nature of the adsorbent used. In the case of a solid–liquid system [32], the role of the agitation is to homogenise the distribution of particles in suspension in the liquid phase and to increase the diffusion of the particles [33], which explains the increase in the yield of the Cerium Ce^{+3} ions during strong agitation.

3.2.2. Effect of the Ce^{+3} initial concentration

A study of the effect of the initial concentration of Ce^{+3} on the adsorption of Ni/Al-ACHPA was carried out with a mass of the support equal to 0.1 g in 10 ml of the aqueous solution at room temperature ($25 \pm 2^\circ C$) by varying the initial concentration of Ce^{+3} (Figure 7) .

Figure 7(b) shows initial Ce^{+3} concentration effect on the adsorption process. We note that for high concentrations of the pollutant, the adsorption efficiency decreases and this can be explained by adsorbent surface saturation of our hybrid material (Ni/Al-ACHPA) [34,35].

3.2.3. pH effect

Monitoring of the variation in the pH of Ce^{+3} in different solutions over time in the presence of Ni/Al-ACHPA studied, will allow us to have an overview of the mechanisms involved during the adsorption of Ce^{+3} . The effect of the power of hydrogen pH on the yield of the extraction of Ce^{+3} cations by Ni/Al-ACHPA created a strong adsorption competition between the cations of Ce^{+3} and the protons of hydrogen H^+ (Figure 7). The more hydrogen power decreases, the more the yield increases, that is to say at basic pH the yield improves. In addition, it is noted that the layered double hydroxides are unstable in acidic media, which explains the low retention rate at $pH = 2$ [36,37].

3.2.4. Effect of the amount of hybrid material (Ni/al-ACHPA)

In order to optimise all the parameters influencing the elimination of Ce^{+3} on the prepared hybrid material Ni/Al-ACHPA, the effect of the concentration of the support on the extraction yield has a very important role in being able to find a better solid/liquid ratio. For this purpose, we have chosen four masses of the support: 0.1, 0.2, 0.3 and 0.5 g. The results are shown in Figure 7. The mass of 0.5 g of adsorbate is the one that best extracts our pollutant. The clogging phenomenon (pasty form) of LDH under the effect of stirring inhibits extraction. This is justified by the increase in the number of adsorption sites of our hybrid material Ni/Al-ACHPA.

3.3. Adsorption isotherm

Adsorption isotherms are functional expressions that describe the adsorbents' equilibrium performance at a given temperature [38,39]. Several theoretical models have been developed to describe adsorption isotherms during an adsorption study. However, in this study, we will only be interested in the models of Langmuir and Freundlich, because they

are the simplest and the most widespread. These adsorption isotherms can be obtained by graphing $Q_e = f(C_e)$.

Q_e is the quantity of substrate adsorbed per gram of adsorbent

C_e is the concentration at equilibrium

3.3.1. Langmuir isotherm

The Langmuir isotherm in the liquid phase is given by:

$$\frac{Q_e}{Q_m} = \frac{K_L C_e}{1 + K_L C_e} \quad (1)$$

This equation has been processed in its linearised form, known as Langmuir 1:

$$\frac{1}{Q_e} = \frac{1}{Q_m} + \frac{1}{Q_m K_L} \frac{1}{C_e} \quad (2)$$

With:

Q_e : the adsorption capacity at equilibrium (mg.g^{-1})

Q_m : the maximum adsorption capacity (mg.g^{-1})

K_L : the adsorption equilibrium constant (Langmuir constant) (L.mol^{-1})

C_e : the concentration of the solute at equilibrium (mol.l^{-1})

By plotting the graph $1/Q_e$ as a function of $1/C_e$ to represent **Figure 8** which represents the Langmuir isotherm of the extraction of Ce^{+3} ions by Ni/Al-ACHPA. The linearised Langmuir equation allows the determination of two important parameters of adsorption, namely the best adsorption capacity (Q_m) and the adsorption equilibrium constant (K_L), from the intercept and the slope, respectively.

$$1/Q_m = 0.099 \text{ and } 1/Q_m.K_L = 13.334$$

3.3.2. Freundlich isotherm

The Freundlich equation is an empirical equation widely used for the practical representation of the adsorption equilibrium. It comes in the form:

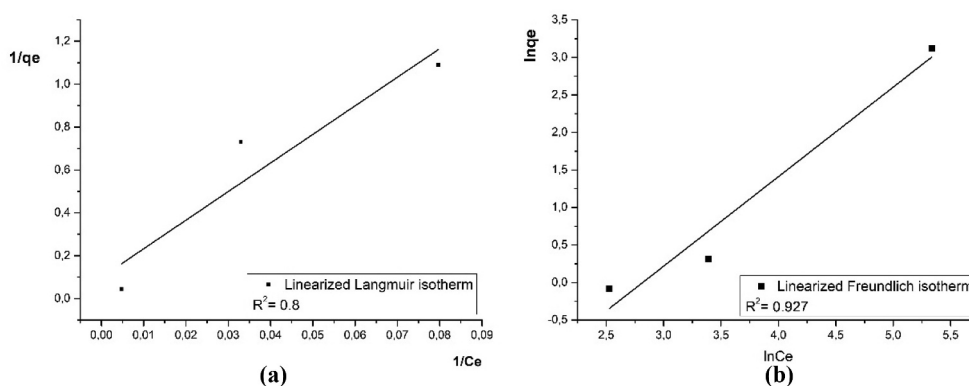


Figure 8. Adsorption isotherm: (a) Langmuir isotherm, (b) Freundlich isotherm.

$$Q = KC_e^{\frac{1}{n}} \quad (3)$$

With

Q: Amount adsorbed per gram of solid

C_e: Concentration of adsorbate at adsorption equilibrium

K and **1/n:** Constants characterising the efficiency of a given adsorbent with respect to a given solute.

The linear transform makes it possible to check that the validity of Equation (3) is obtained by switching to a logarithmic scale:

$$\ln Q_e = \ln K + \frac{1}{n} \ln C_e \quad (4)$$

This equation is that of a line with slope 1/n and ordinate at the origin log (K). In general, (n) is between 0.8 and 2 and is proportional to the strength of adsorption (Figure 8).

So:

We have found $\frac{1}{n} = 1,19 > 1$

In this case, we can say that it is a strong adsorption of Ce⁺³ on Ni/Al-ACHPA.

According to the study of the two isotherms: linearised Langmuir isotherm (R² = 0.8) and linearized Freundlich isotherm (R² = 0.927) for the process of adsorption of Ce⁺³ ions, the Freundlich isotherm confirms this extraction.

The adsorption process follows the Freundlich isotherm model, and this means that the surface containing the adsorbing sites is a perfectly flat plane with no corrugations (assume the surface is homogeneous), the pollutant is adsorbed in an immobile state, and the adsorption sites are all energetically equivalent [40].

3.4. Kinetic study

The study of the adsorption kinetics of Ce⁺³ on Ni/Al-ACHPA made it possible to specify the order of the reaction. Indeed, we applied two kinetic models, a pseudo-first order model and a pseudo-second order model. By comparison, of the regression coefficients of the curves corresponding to the two kinetic models, we found that those of the second-order models are closest to unity (pseudo-first order model R² = 0.906 and pseudo-second-order model R² = 0.998). We can therefore say that the kinetics of the adsorption reaction of Ce⁺³ on grafted LDH are very probably of the second order (Figure 9).

4. Conclusion

This research sought to eliminate the need for organic solvents by using a good chelating agent, such as phosphonic acids, to retain metal cations (i.e. liquid-liquid extraction), by grafting this chelating agent into a solid support and making the solid-liquid extraction. This grafting gave us a new hybrid material Ni/Al-ACHPA, which forced us to characterise it by different characterisation methods and to study these adsorptive characteristics vis-à-vis inorganic pollutants. This study demonstrates Ni/Al-ACHPA efficiency in eliminating Ce⁺³ ions in an aqueous medium. The influence of parameters related to operating conditions was examined. The kinetic study shows that equilibrium is

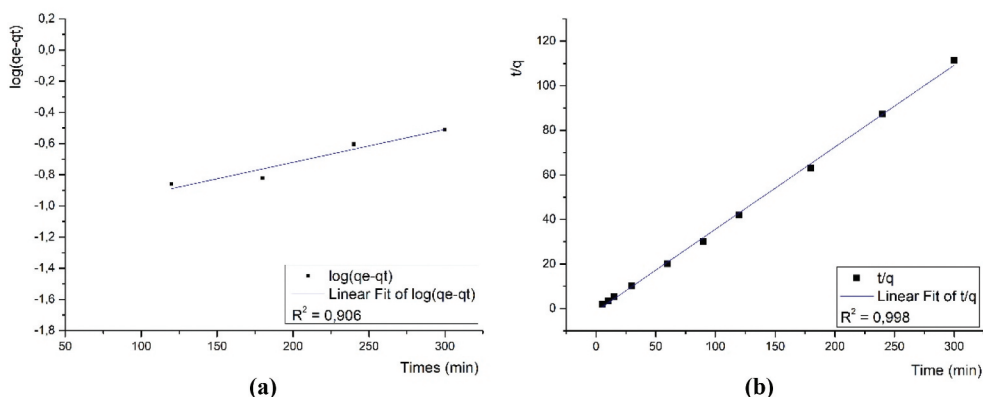


Figure 9. Kinetic study, (a) pseudo-first order, (b) pseudo-second order.

established after less than 30 min and that the adsorption mechanism can be described by pseudo-second-order kinetics. The plot of the adsorption isotherms shows that the Freundlich model perfectly represents the adsorption. Ni/Al-ACHPA was found to be a support that has a generally high adsorption affinity towards Ce^{+3} ions. This work gives us the opportunity to synthesise other hybrid materials by grafting organic compounds into the inter-sheet space of double lamellar hydroxides in order to study their adsorptive properties in general.

Disclosure statement

No potential conflict of interest was reported by the author(s).

ORCID

M. Kadari  <http://orcid.org/0000-0002-7522-9593>
M. Makhlouf  <http://orcid.org/0000-0002-6157-5073>
Z. Benmaamar  <http://orcid.org/0000-0001-9469-7301>
D. Villemin  <http://orcid.org/0000-0002-6266-3817>

References

- [1] Han X, Zhang X-Q, Yang S-Q, et al. The effects of scale inhibitor ATMP in water on nanofiltration. *Desalin Water Treat.* **2019**;160:913.
- [2] Yin W, Liu L, Zhang H, et al. A facile solvent-free and one-step route to prepare amino-phosphonic acid functionalized hollow mesoporous silica nanospheres for efficient Gd(III) removal. *J Clean Prod.* **2020** January 10;243:118688.
- [3] Lindenberg MA, Retèl VP, van den Berg JH, et al. Treatment with tumor-infiltrating lymphocytes in advanced melanoma: evaluation of early clinical implementation of an advanced therapy medicinal product. *J Immunother.* **2018** novembre;41(9):41325.
- [4] Rott E, Steinmetz H, Metzger JW. Organophosphonates: a review on environmental relevance, biodegradability and removal in wastewater treatment Plants. *Sci Total Environ.* **2018** février;615:117691.

- [5] Horiguchi M, Kandatsu M. Isolation of 2-aminoethane phosphonic acid from rumen protozoa. *Nature*. 1959 septembre;184(4690):9012.
- [6] Liu C, Ai G, Song S. The effect of amino trimethylene phosphonic acid on the flotation separation of pentlandite from lizardite. *Powder Technol*. 2018 août;336:52732.
- [7] Šolínová V, Mikysková H, Maxmilián Kaiser M, et al. Estimation of apparent binding constant of complexes of selected acyclic nucleoside phosphonates with β -cyclodextrin by affinity capillary electrophoresis: CE and CEC. *Electrophoresis*. 2016 janvier;37(2):23947.
- [8] Amine Didi M, Kaid M, Villemin D. Dodecylhydroxydiphosphonic acid for solvent extraction. *Solvent Extr Ion Exch*. 2008 mars;26(2):11327.
- [9] Uzma N, Khaja Mohinuddin Salar BM, Kumar BS, et al. Impact of organic solvents and environmental pollutants on the physiological function in petrol filling workers. *Int J Environ Res Public Health*. 2008;5(3):139–146.
- [10] Zhu S, Asim Khan M, Wang F, et al. Rapid removal of toxic metals Cu^{2+} and Pb^{2+} by amino trimethylene phosphonic acid intercalated layered double hydroxide: a combined experimental and DFT study. *Chem Eng J*. 2020;392:123711.
- [11] Ren Q, Wang G, Wu T, et al. Calcined MgAl-layered double hydroxide/graphene hybrids for capacitive deionization. *Ind Eng Chem Res*. 2018 mai 9;57(18):641725.
- [12] Gore CT, Omwoma S, Chen W, et al. Interweaved LDH/PAN nanocomposite films: application in the design of effective hexavalent chromium adsorption technology. *Chem Eng J*. 2016 janvier;284:794801.
- [13] Mohamed Kadari MK, Ben Ali M, Villemin D. The intercalation of Zn/Al-HDL by the diamino-dodecylphosphonic acid: synthesis and properties of adsorption of basic fuchsin. *J Chin Adv Mater Soc*. 2016;4(2):148–157.
- [14] Miyata S. The syntheses of hydrotalcite-like compounds and their structures and physico-chemical properties I: the systems Mg^{2+} - Al^{3+} - NO_3^- , Mg^{2+} - Al^{3+} - Cl^- , Mg^{2+} - Al^{3+} - ClO_4^- , Ni^{2+} - Al^{3+} - Cl^- and Zn^{2+} - Al^{3+} - Cl^- . *Clays Clay Miner*. 1975;23(5):36975.
- [15] Prasanna SV, Kamath PV. Anion-exchange reactions of layered double hydroxides: interplay between coulombic and H-bonding interactions. *Ind Eng Chem Res*. 2009 juillet 1;48(13):631520.
- [16] Kuroda Y, Oka Y, Yasuda T, et al. Precise size control of layered double hydroxide nanoparticles through reconstruction using tripodal ligands. *Dalton Trans*. 2018;47(37):1288492.
- [17] Jaishankar M, Tseten T, Anbalagan N, et al. Toxicity, mechanism and health effects of some heavy metals. *Interdiscip Toxicol*. 2014 juin 1;7(2):6072.
- [18] Chen H, Zhou Y, Wang J, et al. Polydopamine modified cyclodextrin polymer as efficient adsorbent for removing cationic dyes and Cu^{2+} . *J Hazard Mater*. 2020 mai;389:121897.
- [19] Foroutan R, Peighambaroust SJ, Ahmadi A, et al. Adsorption mercury, cobalt, and nickel with a reclaimable and magnetic composite of hydroxyapatite/ Fe_3O_4 /polydopamine. *J Environ Chem Eng*. 2021 août;9(4):105709.
- [20] Foroutan R, Peighambaroust SJ, Mohammadi R, et al. Development of new magnetic adsorbent of walnut shell ash/starch/ Fe_3O_4 for effective copper ions removal: treatment of groundwater samples. *Chemosphere*. 2022 juin;296:133978.
- [21] Torab-Mostaedi M. Biosorption of lanthanum and cerium from aqueous solutions using tangerine (*Citrus reticulata*) peel: equilibrium, kinetic, and thermodynamic studies. *Chem Ind Chem Eng Q*. 2013;19(1):7988.
- [22] Najafi Lahiji M, Reza Keshkar A, Ali Moosavian M. Adsorption of cerium and lanthanum from aqueous solutions by chitosan/polyvinyl alcohol/3-mercaptopropyltrimethoxysilane beads in batch and fixed-bed systems. Part Sci Technol. 2018;36(3):340–350.
- [23] Silverstein RM, Basler GC, Morill TC. Identification spectrométrique de composés organiques. Bruxelles: Edition De Boeck et Larcier; 1998. p. 91–92.
- [24] Romanzini D, Piroli V, Frache A, et al. Sodium montmorillonite modified with methacryloxy and vinylsilanes: influence of silylation on the morphology of clay/unsaturated polyester nanocomposites. *Appl Clay Sci*. 2015 septembre;114:55057.

- [25] Funnell NP, Wang Q, Connor L, et al. Structural characterisation of a layered double hydroxide nanosheet. *Nanoscale*. 2014;6(14):803236.
- [26] Hobbs C, Jaskaniec S, McCarthy EK, et al. Structural transformation of layered double hydroxides: an in situ TEM analysis. *Npj 2D Mater Appl*. 2018 décembre;2(1):4.
- [27] Rajendran S, Apparao B, Palaniswamy N. Synergistic effect of Zn²⁺ and ATMP in corrosion inhibition of mild steel in neutral environment. *Bull Electrochem*. 1996;12:15–19.
- [28] Thi Xuan Hang T, Truc TA, Hoai Nam T, et al. Corrosion protection of carbon steel by an epoxy resin containing organically modified Clay. *Surf Coat Technol*. 2007 mai;201(16–17):740815.
- [29] González M, Pavlovic I, Rojas-Delgado R, et al. Removal of Cu²⁺, Pb²⁺ and Cd²⁺ by layered double hydroxide–humate hybrid. Sorbate and sorbent comparative studies. *Chem Eng J*. 2014;254:605–611.
- [30] Kadari M, Kaid M, Ben Ali M, et al. Selective study of elimination of Cd (II) and Pb (II) from aqueous solution by novel hybrid material. *J Chin Adv Mater Soc*. 2017 juillet 3;5(3):14957.
- [31] Kuśmierk K, Świątkowski A. The influence of different agitation techniques on the adsorption kinetics of 4-chlorophenol on granular activated carbon. *React Kinet Mech Catal*. 2015 octobre;116(1):26171.
- [32] Mixing in solid–liquid systems. In: *Solid-liquid two phase flow*. Elsevier; 2008. p. 385438. DOI:10.1016/B978-044452237-5.50009-6
- [33] Hamzezadeh A, Rashtbari Y, Afshin S, et al. Application of low-cost material for adsorption of dye from aqueous solution. *Int J Environ Anal Chem*. 2022 janvier 2;102(1):25469.
- [34] Panda H, Tiadi N, Mohanty M, et al. Studies on adsorption behavior of an industrial waste for removal of chromium from aqueous solution. *S Afr J Chem Eng*. 2017 juin;23:13238.
- [35] Ndi Nsami J, Mbadcam JK. The adsorption efficiency of chemically prepared activated carbon from cola nut shells by on methylene blue. *J Chem*. 2013;2013:17.
- [36] Chen R, Hung S, Zhou D, et al. Layered structure causes bulk nife layered double hydroxide unstable in alkaline oxygen evolution reaction. *Adv Mater*. 2019 octobre;31(41):1903909.
- [37] Nestroinaia OV, Ryltsova IG, Lebedeva OE. Effect of synthesis method on properties of layered double hydroxides containing Ni(III). *Crystals*. 2021 novembre 21;11(11):1429.
- [38] Yao B, Zhi D, Zhou Y. Iron-based materials for removal of arsenic from water. In: *Sorbents materials for controlling environmental pollution*. Vol. 20945. Elsevier; 2021. DOI:10.1016/B978-0-12-820042-1.00025-0
- [39] Lofrano G, Carotenuto M, Libralato G, et al. Polymer functionalized nanocomposites for metals removal from water and wastewater: an overview. *Water Res*. 2016 avril;92:2237.
- [40] Azizian S, Eris S. Adsorption isotherms and kinetics. In: *Interface science and technology*. Vol. 33. Elsevier; 2021. p. 445509. DOI:10.1016/B978-0-12-818805-7.00011-4